ORGANIC PROCESS RESEARCH & DEVELOPMENT
OPR&D
Article
pubs.acs.org/OPRD

Continuous Processing and Efficient *in Situ* Reaction Monitoring of a Hypervalent Iodine(III) Mediated Cyclopropanation Using Benchtop NMR Spectroscopy

Batool Ahmed-Omer,*[,†] Eric Sliwinski,[†] John P. Cerroti,[‡] and Steven V. Ley[†]

[†]Department of Chemistry, University of Cambridge, Lensfield Road, Cambridge CB2 1EW, U.K.
[‡]Magritek GmbH, Gebäude VO (Building VO), Triwo Technopark Aachen, Philipsstrasse 8, 52068 Aachen, Germany

Supporting Information

ABSTRACT: Real-time NMR spectroscopy has proven to be a rapid and an effective monitoring tool to study the hypervalent iodine(III) mediated cyclopropanation. With the ever increasing number of new synthetic methods for carbon−carbon bond formation, the NMR *in situ* monitoring of reactions is becoming a highly desirable enabling method. In this study, we have demonstrated the versatility of benchtop NMR using inline and online real-time monitoring methods to access mutually complementary information for process understanding, and we developed new approaches for real-time monitoring addressing challenges associated with better integration into continuous processes.

INTRODUCTION

The understanding, quality, and control of chemical processes are of vital importance from early discovery through to process optimization and scale-up onto full scale manufacturing. Chemical manufacturing, in fact, dictates the need for significant resources and effort to be invested in processes knowledge at an early stage to increase business efficiency.[1] Similarly, the quality-by-design approach to chemical synthesis relies on the knowledge acquired by process monitoring for control and risk minimization at source.[2] This is best achieved by monitoring the chemical processes using a basis of real-time analytics. Similarly, integrating real-time analysis is fundamental to delivering the green chemistry agenda.[3] In this respect, the application of process analytical technologies (PAT) is an established approach for compliance across a number of industries.[4] Furthermore, the reliance on appropriate technologies for efficient data processing in real-time becomes ever more apparent. In fact, the acquisition of large data is of little value without suitable tools to extract the crucial knowledge. Hence multivariate data processing along with other statistical tools and intelligent algorithms are already being applied to data analysis.[5] On the other hand, the "Internet of Things" is a revolution already underway, based on a vision in which every element of a process is connected via network, allowing continuous data exchange in real time. This entails significant revenue opportunities for research and process manufacturing integrated with real-time analytics, an area which is expected to significantly impact and grow over the following years. Approaches based on continuous flow process have addressed a number of inherent synthesis challenges over the decades, owing to its well-established benefits and amenability toward automation. Likewise, the potential for new understanding of reaction processes can be realized when fully integrated with appropriate analytics. Recent studies, in fact, have shown the application of flow technologies with real-time analysis offering an insight into intelligent reaction optimization.[6] In the recent years, the improvements in analytical technologies by achieving enhanced sensitivity, improved acquisition and sampling techniques have progressively presented a greater efficiency. Techniques, such as mass spectrometry and infrared spectroscopy, are increasingly being applied for *in situ* reaction monitoring.[7] Among these methods, the inherent versatility of nuclear magnetic resonance (NMR) spectroscopy enables simultaneous structure identification and quantification in process understanding, therefore the demand for rapid reaction monitoring using NMR spectrometers is significantly on the increase.[8] The recent development of compact NMR spectroscopy, based on high-homogeneity permanent magnet designs, has enabled NMR to emerge as a convenient analytical and quality control tool with improved sensitivity for process study of both batch and flow reactions.[9] In the work reported below we demonstrate the potential and reliability of benchtop NMR as an *in situ* monitoring tool for continuous processing employing inline and online methods. In the study, we have developed a continuous flow process that is fully integrated with benchtop NMR technology for a hypervalent iodine(III) mediated cyclization to generate substituted cyclopropanes. Real-time monitoring using the benchtop NMR for this study proved to be an ideal informative analytical tool for cyclopropanation due to its distinctive spectral features. In this application we also successfully developed an inline solvent switching device to aid the monitoring process. Moreover, automated scripting was developed to expand on the NMR monitoring capabilities by generating sequences of both one and two-dimensional homonuclear proton NMR experiments. This enabled us to study the evolution of the distinctive coupling relationships of cyclopropane protons over time when using 2D correlation spectroscopy (COSY) and *J*-resolved spectroscopy (*J*-RES). Finally, we have also integrated compact

Received: May 19, 2016
Published: August 10, 2016

DOI: 10.1021/acs.oprd.6b00177
Org. Process Res. Dev. 2016, 20, 1603−1614

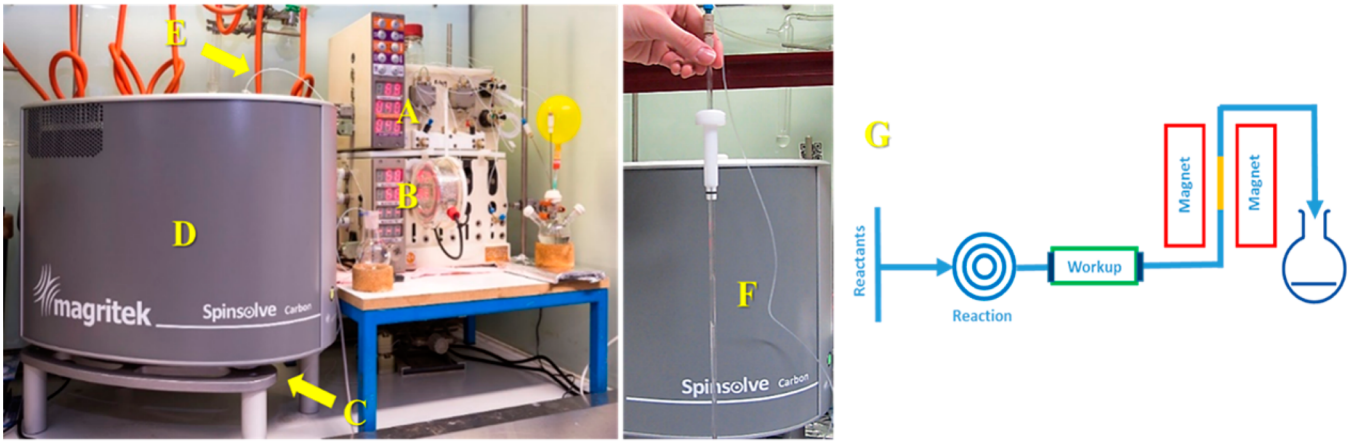

Figure 1. Default setup for reaction monitoring with Spinsolve benchtop NMR integrated with Vaportec R2+/R4 flow system (left). Glass NMR flow cell placed outside the NMR bore (middle). Reaction monitoring configuration (right). Legend: (A) Vaportec R2+ double pump unit. (B) Vaportec R4 flow reactor unit. (C) Flow stream input into the benchtop NMR. (D) Benchtop NMR. (E) Flow stream output from the NMR tube. (F) Glass NMR flow cell. (G) Inline reaction monitoring configuration under continuous flow conditions.

mass spectrometry into the inline NMR setup, demonstrating a complementary approach to multiple monitoring technique to provide additional insights into our process understanding.

REACTION MONITORING SYSTEM AND METHODS

2.1. The Benchtop NMR System. Reaction monitoring in this study was based on proton NMR measurements carried out using the Spinsolve benchtop NMR spectrometer, designed by Magritek and built with a permanent magnet based on a Halbach design, working at a frequency of 43.62 MHz. The benchtop NMR has a vertical through-bore that runs from top to bottom of the device. This allows measurements to be made using two types of NMR flow cells: (i) PTFE tubing inserted into a glass cell guide to center the tubing through the NMR bore, and (ii) glass NMR flow cell tube designed to provide an enlarged sample volume at the NMR measurement zone, thus maximizing sensitivity, while minimizing volume elsewhere.[10] In this work, the glass NMR flow cell was primarily used unless otherwise stated. For continuous flow process, the benchtop NMR was integrated with the Vaportec R2+/R4 flow system as illustrated in Figure 1. During a typical experiment, the flow output was streamed through the glass NMR cell. The benchtop NMR can be interfaced with the Spinsolve software, where the collected data are displayed and processed using MNOVA in real-time, including automatic spectrum baseline correction and phasing.

2.2. Reaction Monitoring Methodologies. For the purpose of our reaction monitoring studies, two main approaches were adopted using both one and two-dimensional proton NMR experiments, namely inline monitoring and online monitoring.[11] The inline approach, was based on subjecting the continuous flow reaction stream to a series of proton NMR measurements, with acquisitions typically between 0.4 to 6.4 s, to profile the steady-state of the flow reaction and obtain information on the flow stream composition (Figure 1). With this method, the continuous process gives the intrinsic advantage of allowing a sequential varying of reaction conditions, better established when dispersion of concentration gradient is minimized between reaction runs.

In this study, we further integrated the inline methodology with the solvent evaporation device between the flow outlet and the benchtop NMR, in order to allow the switching from reaction to analytical medium, hence recording spectra in a semideuterated media (*vide infra*). On the other hand, the online monitoring of reaction approach allowed for tracking the reaction progress with respect to changes in reactant or product concentration occurring over time. The reaction was carried under batch using the R4 glass reactor, easily accommodated into the Vaportec R4 unit holder, coupled with the benchtop NMR system as illustrated in Figure S2 of Supporting Information. Circulation of the reaction stream from the R4 glass reactor and through the NMR magnet zone was achieved by using a Reglo digital peristaltic pump, allowing measurements at desired intervals. The online approach was found to be a convenient method for observing the reaction progress over time, while making use of the relatively low reaction volume with the advantage of the intrinsic reaction consistency given by the use of one single stock solution under unperturbed state. For both inline and online methods, optimal flow rates were evaluated with respect to the mixture's concentration in order to ensure effective acquisition of the magnetized section of the flow stream to enhance the signal-to-noise ratio. Reaction times reported for all reactions in this work take into account the time necessary for the solution transfer between reaction chamber and NMR detection zone, given by the volume divided by flow rate. NMR spectra timeline, however, correspond to the software measurement times, which is manually activated with the first sample aliquot reading.

2.3. Solvent Switching System. Compared to high-field NMR, the fast automatic hardware lock using an external lock configuration of the benchtop NMR allows the utilization of nondeuterated solvent. However, the need to carry analysis in deuterated media may still be desirable in cases where the reaction's solvent and its satellite signals found to obscure areas of interest in the NMR spectrum. This was the case in some of our monitoring experiments, and hence the need to integrate a solvent switching step while enabling uninterrupted reaction-to-analysis process was realized. Although continuous solvent removal and switching is widely used on an industrial scale as well as on microfluidic scales, however, there is a growing demand for continuous evaporation techniques in discovery laboratory scales to facilitate downstream processing. Recently, we reported a convenient and efficient prototype device for evaporation, concentrating, and switching solvents in continu-

DOI: 10.1021/acs.oprd.6b00177
Org. Process Res. Dev. 2016, 20, 1603−1614

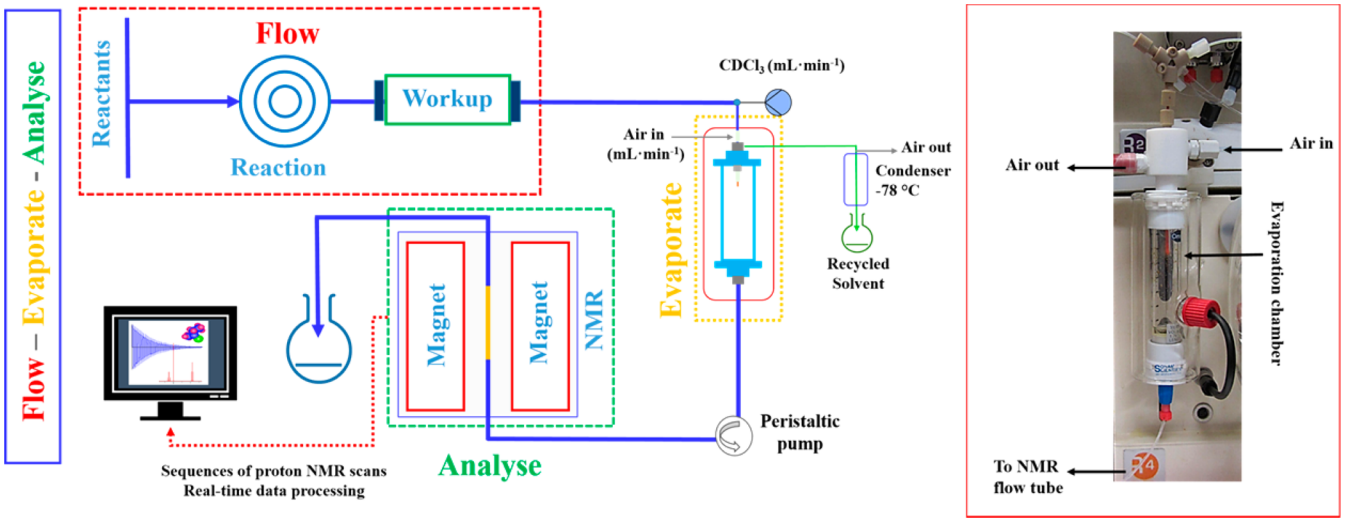

Figure 2. Flow-evaporate-analyze operation setup.

ous flow.[12] This simple and robust prototype was constructed from commercially available parts, and developed based on exposure of a high surface spray of solution to a desolvating gas stream, removing solvent quickly and efficiently, and compatibly with the existing flow chemistry equipment. Key parameters affecting the solvent switching, such as the sprayer dimensions, were studied and optimized. In this work, an in-house modified version of the initial prototype solvent evaporation system was used, based on a polymeric spraying device with a more compact assembly, minimizing the amount of components necessary for replacement and ease of servicing. This modified solvent evaporation device consists of two blocks of chemically resistant PTFE attached by a single threaded screw, and fitted into a standard Omnifit glass column acting as the evaporation chamber, as illustrated in the Supporting Information section (Figure S5). The final assembly could easily accommodate on a Vaportec R4 heating jacket. The switching process was configured to allow for a complete integrated operation of flow-evaporate-analyze protocol, i.e., carrying out flow reaction, then evaporate, and switch to deuterated solvent, followed by direct NMR analysis (Figure 2). During the switching operation, the continuous reaction output was pumped into the evaporation device, while the desolvating air stream was maintained at an optimal flow rate allowing for spray formation in the chamber. Deuterated chloroform was then pumped into the device's chamber and the resulting diluted crude mixture was streamed into the benchtop NMR using the peristaltic pump. Parameters for the solvent evaporation and switching were initially optimized based on a dichloromethane (DCM) and chloroform ($CHCl_3$) system, mimicking the reaction medium and deuterated solvent, respectively. The optimization study was carried out according to a set of variables, namely (a) DCM and chloroform solvent flow rates, (b) chloroform solvent time of injection, (c) gas streamflow rate, and (d) evaporation chamber temperature. The optimum set of conditions led to a satisfactory 97:3 $CHCl_3$:DCM ratio monitored by the benchtop NMR (Table S2 and Figures S8 and S9)

RESULTS AND DISCUSSION

3.1. Online Monitoring of Malononitrile 1 Cyclopropanation Reaction Progress. The cyclopropanation reaction of olefins with malononitrile in the presence of $PhI(OAc)_2$ (diacetoxyiodobenzene or DIB) gives access to a range of 1,1-dicyanocyclopropane derivatives under mild oxidative conditions. Compared with other common routes to substituted cyclopropyl substrates, this method has the advantage of not requiring the use of transition metal catalysis, thus making the process cleaner and avoiding additional scavenging steps. To initiate the reaction monitoring study we selected the direct preparation of 1,1-dicyanocyclopropane **3** derived from the activated methylene malononitrile **1** and 4-*tert*-butylstyrene **2** (Scheme 1), based upon literature

Scheme 1. Hypervalent Iodine(III) Mediated Synthesis of 1,1 Dicyanocyclopropane 3

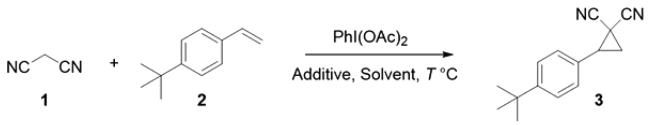

precedents on the DIB mediated cyclopropanation first reported by Wirth et al., and later by Zhang et al.[13,14] It was observed that the optimized batch conditions of the reaction required an inert atmosphere, and replacing molecular oxygen with DIB to obtain the cyclopropane moiety exclusively while suppressing the hydro-cyanation of the olefin substrate.

The initial selection of a system for real-time monitoring studies found that reacting 4-*tert*-butylstyrene **2** with malononitrile **1**, in excess DIB and K_2CO_3 in 1,2-dichloroethane (DCE) at 50 °C afforded cyclopropane **3** in good yield (82%) and over a relatively short time (2 h.). Having therefore found satisfactory reaction conditions, we set out to investigate the reaction progress over time using the online method as previously described (Figure S2). In order to prevent any potential blockages, we segregated the heterogeneous K_2CO_3 from the circulating stream using a filter at the reactor outlet. This filtration will also avoid the perturbation of the NMR field homogeneity if a heterogeneous stream passes through the NMR detection zone. Although the benchtop NMR exhibit an external lock feature, the reaction was nevertheless carried out in deuterated chloroform for greater spectrum clarity. The reaction mixture was continuously circulated through the NMR detection zone to carry out a series of 1D proton NMR

DOI: 10.1021/acs.oprd.6b00177
Org. Process Res. Dev. 2016, 20, 1603−1614

measurements in intervals. Due to the absence of heating and the need for K_2CO_3, we assumed that the reaction does not advance significantly in the path between reaction bulk and NMR detection zone. Measurements were then taken at the intervals of 14, 18, 23, 26, 30, and 47 min, representing a good monitoring window to observe product formation as predominant, generating a total of six stacked spectra to profile the reaction progress as shown in Figure 3a. With each

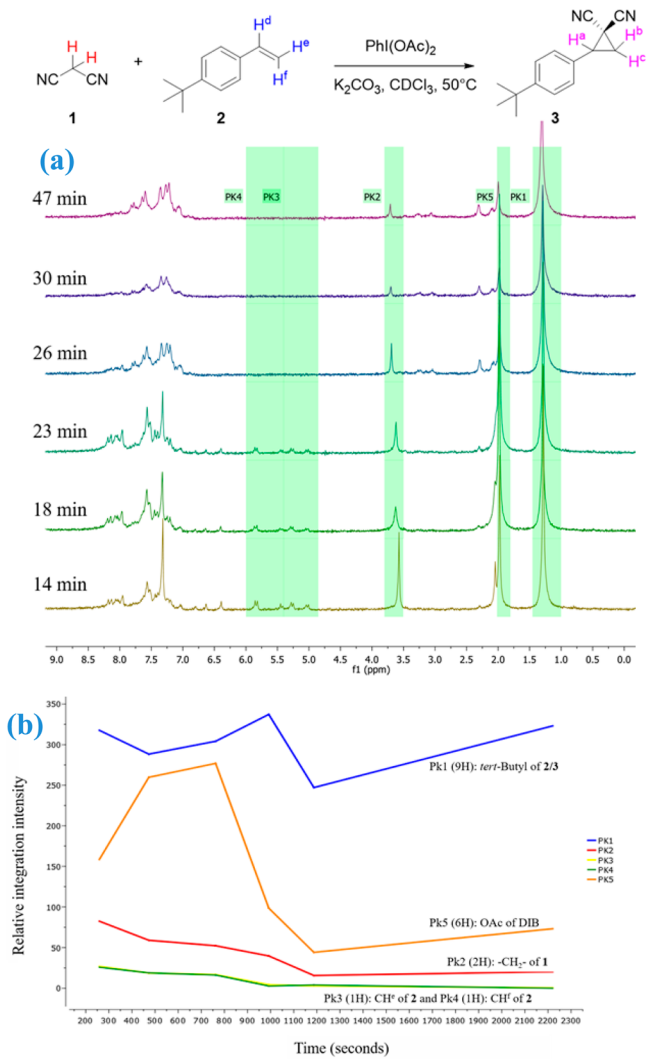

Figure 3. Online monitoring of the cyclopropanation reaction of **1** with **2** using Spinsolve benchtop NMR (43 MHz): (a) ^{1}H NMR array plot from 14 to 47 min reaction time. (b) Profile of reaction progress acquired using the ^{1}H NMR data referenced to selected resonances.

measurement, integration values of five selected resonances on the spectrum, were automatically derived by the MNOVA software (Figure 3b). From both representations in Figure 3, we were able to monitor the consumption of the limiting reactant styrene **2** and the formation of the cyclopropane adduct **3**. As profiled in Figure 3a, the starting material **1**, **2**, and DIB were predominantly present at the initial measurement at 14 min reaction time. Within 26 min, the majority of the styrene **2** was consumed, coinciding with the appearance of the distinctive peaks of the vicinal CH^a of cyclopropane **3** (δ_H 3.1−3.6) and the geminal H^c−C−H^b (δ_H 2.2−2.5). Progressive disappearance of starting materials malononitrile and DIB was also successfully detected by monitoring of peaks Pk2 and Pk5, while the chemical shift of Pk1, on the other hand, did not change overall, due to the presence of the *tert*-butyl moiety on both the styrene **2** and the adduct **3**. Moreover, the progress profile of the cyclopropanation reaction in Figure 3b, acquired from the ^{1}H NMR measurements, gave a visual and quantitative account of reagent consumption and product formation, with respect to selected resonances, expressed as relative integration vs. time coordinate. The clear advantage of such type of output is in the numerical values which can be used as triggers during computer controlled processes, for instance, in order to suppress alternative reaction pathways or in defining optimal process times. In the progress profile shown in Figure 3b, however, oscillation of the recorded chemical shift intensity trends were observed. This is especially noticeable for Pk1 which corresponds to the *tert*-butyl moiety present in both substrate **2** and product **3**, as opposed to the expected constant progress trend. This fluctuation in NMR signal intensity is likely caused by the flow turbulences created due to the peristaltic pumping mechanism as well as the enlargement of the NMR flow cell at the measurement zone. It is important to point out that both representations shown in Figure 3, are equally important and beneficial in their own right: the NMR spectra array, although non-numerical, can visually help detect all events including the unexpected ones, whereas the relative integration profile highlights the progress of a preselected resonances.

Furthermore, the monitoring of the cyclopropanation reaction progress of malononitrile **1** with **2** was also correlated with the two-dimensional homonuclear correlation spectroscopy experiments (COSY). The cyclopropane structure lends itself well to this technique, due to the presence of a number of distinctive coupling relationships between its protons. While the use of COSY is traditionally and largely used for detailed characterization purposes, its application as a reaction monitoring tool is becoming increasingly attractive. The traditional 2D COSY NMR has a long acquisition duration, which is considered slow for reaction monitoring purposes. With recent advances in benchtop NMR spectroscopy, however, development of new 2D pulse sequences technology such as Quickcosy has been realized to enable fast and efficient 2D NMR measurements within a single scan at a medium field.[15] We took advantage of the Quickcosy experiment protocol provided by the Spinsolve benchtop NMR, one scan every 10 min, which is more suited for monitoring the progress of cyclopropanation of malononitrile **1** with **2**, to identify the interactions between the coupled protons in the reaction mixture, thus enabling to track the simultaneous formation and disappearance of correlations over time. The measured COSY contour at 5, 16, 27, and 50 min reaction times, displayed a number of diagonal and off-diagonal (cross) correlations representing coupled protons (Figure 4). At 5 min of reaction time, the presence of unreacted styrene **2** substrate was confirmed by the coupling relationship (C1) at δ_H 5.0−7.2, between its geminal H^e−C−H^f and vicinal CH^d. The presence of starting substrates malononitrile **1** and DIB was established simply through the diagonal peaks C2 and C3, due to no coupling interaction within their structures. As the reaction progressed, the correlation peaks for all starting species progressively decreased, while the characteristic cross and diagonal correlation of the cyclopropyl adduct **3** due to the vicinal and geminal coupling interactions (C4 and C5) intensified by 50 min of reaction. The overall observation of

DOI: 10.1021/acs.oprd.6b00177
Org. Process Res. Dev. 2016, 20, 1603−1614

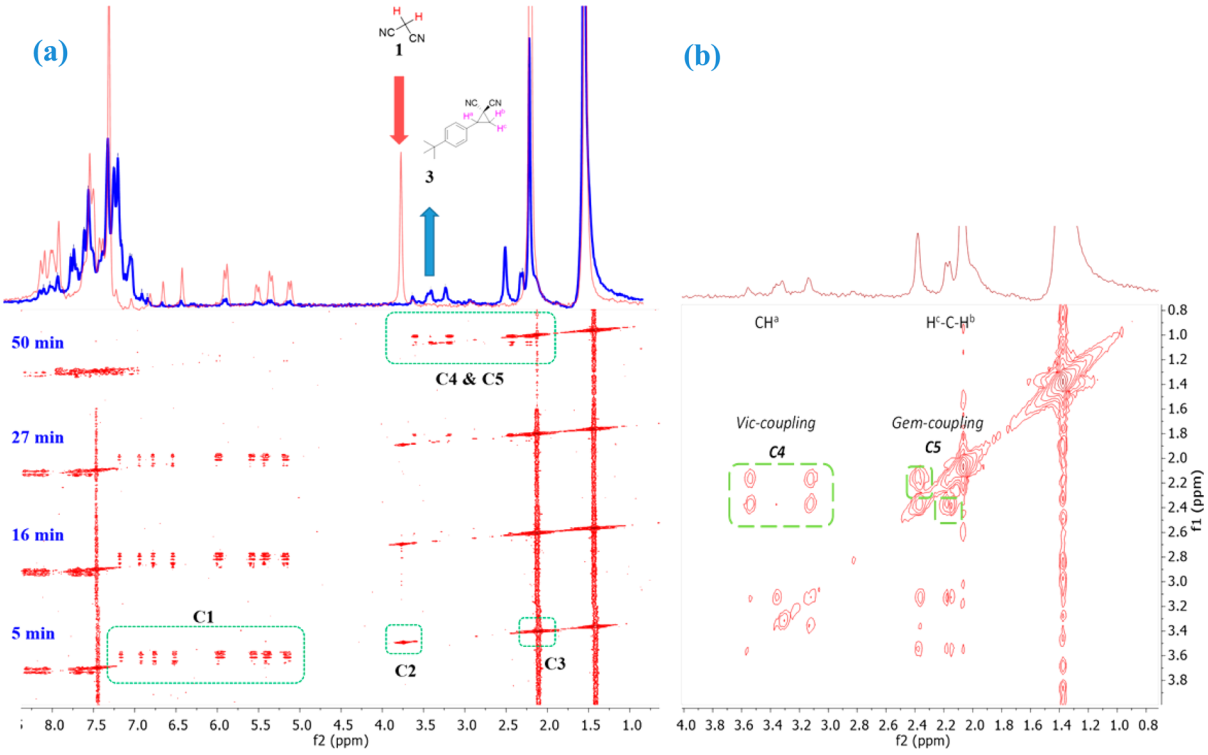

Figure 4. (a) COSY contour array profiling the reaction progression over time of cyclopropanation of **1** using Quickcosy. (b) Close-up region, of reaction monitored at 50 min, between δ_H 0.8−4.0, highlighting the geminal and vicinal correlations.

reactant consumption and progressive appearance of cyclopropane **3** using 2D Quickcosy coincided with that of the 1D ^{1}H NMR. Used in combination with 1D, generally 2D techniques can offer a complementary quantitative, qualitative as well as characterization information on the cyclopropanation progress monitoring of **1**.

3.2. Inline Monitoring of Malononitrile 1 Cyclopropanation under Continuous Process. A continuous flow process for the hypervalent iodine(III) mediated preparation of 1,1-dicyanocyclopropane **3** was developed and configured to allow for a complete continuous operation of the flow-evaporate-analyze protocol as described earlier. This approach allowed us to successfully address one of the major challenges associated with integrating the real-time NMR analysis with flow process. During monitoring of the cyclopropanation reaction, peak identification and integration proved challenging due to the use of a protonated solvent, which obscured some of the spectral features. Using the Vaportec R2+/R4 flow system, the preparation of the cyclopropane **3** under continuous flow conditions was carried out in dichloromethane (DCM) by introducing a 0.30 M solution of malononitrile **1** and styrene **2** along with 0.55 M solution of DIB, through a prepacked column of K_2CO_3, over 44 min residence time (Figure 5). The reaction stream output was then directed to the solvent evaporation device and then into the NMR detection zone. The use of prepacked K_2CO_3 cartridge was found best when mixed with 1 mm sized glass beads, to avoid the agglomeration of the K_2CO_3 salts as the organic reaction media was flowed through the reactor, subsequently blocking the flow stream over time. In addition, the advantage of superheating under flow conditions allowed the use of more volatile DCM in the system instead of the conventional DCE, therefore improving the solvent exchange process. The inline monitoring of malononitrile **1** cyclo-

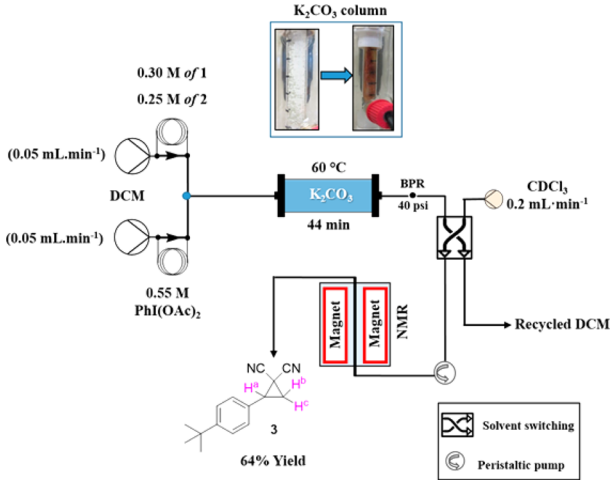

Figure 5. Inline monitoring setup of malononitrile **1** cyclopropanation under flow conditions using the flow-evaporate-analyze protocol.

propanation was carried out using the Spinsolve reaction monitoring protocol (RM), and with each measurement the integration values of selected resonances were extracted to produce a series of trends, representing the selected resonances, to profile the steady-state of the continuous reaction in real-time mode (Figure 6). Upon closer examination of the steady-state profile, it was clear that a significant reaction conversion took place as an increase in the relative integration values of the cyclopropane ring protons of product **3** were observed compared to that of the starting substrates malononitrile **1** and styrene **2**.

3.3. Online Reaction Progress Monitoring of Ethyl-nitroacetate 4 Cyclopropanation. An analogous approach for the online monitoring, as previously described, was

DOI: 10.1021/acs.oprd.6b00177
Org. Process Res. Dev. 2016, 20, 1603−1614

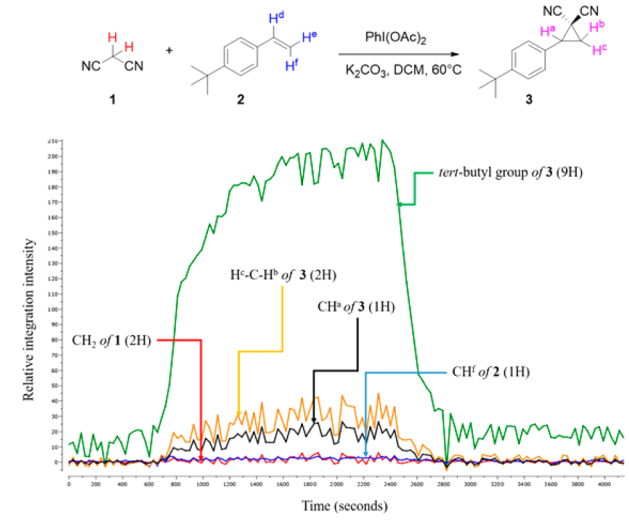

Figure 6. Inline monitoring of cyclopropanation of **1** using Spinsolve benchtop NMR (43 MHz): steady-state profile under flow conditions acquired using the ^{1}H NMR data referenced to selected resonances.

extended to the cyclopropanation of ethyl-nitroacetate **4**. This hypervalent iodine(III) mediated cyclization provides access to a range of 1-nitro-1-cyclopropyl carboxylates which are valuable synthetic building blocks ultimately leading to cyclopropane α-amino acids.[16] In order to exemplify further the use of the benchtop NMR, we selected the preparation of cyclopropane carboxylate **5** derived from the ethyl-nitroacetate **4** and 4-*tert*-butylstyrene **2** (Scheme 2). As a suitable candidate, the

Scheme 2. Hypervalent Iodine(III) Mediated Synthesis of Ethyl-1-nitro-2(4-*tert*-butyl)-cyclopropane Carboxylate 5

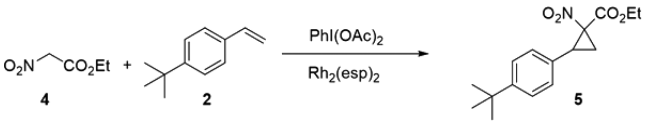

cyclization was carried out using the conditions based on the work of Charette et al., to generate iodonium ylide *in situ* from the α-nitroesters which subsequently undergoes cyclopropanation with olefins via the generated carbene in the presence of Rh(II) catalyst.[17]

In initial experiments, we reacted ethyl-nitroacetate **4** in 5-fold excess of styrene **2** at an ambient temperature in the presence of 1.1 equiv DIB and catalytic amounts of *bis*-(rhodium-(α, α, α', α'-tetramethyl-1,2-benzenedipropionica-cid) $Rh_2(esp)_2$, providing the cyclopropane carboxylate **5** in moderate yield (73%) with *E*:*Z* ratio of 5:1 (in substituted cyclopropane isomer *E* indicates a *trans* relationship between the vicinal nitro and aryl group, whereas *Z* indicates the *cis* relationship).

The use of styrene **2** in excess in solvent-less conditions, however, was undesirable with the monitoring study, therefore we aimed at reducing the amount of styrene **2** to an equimolar ratio, in the presence of an equivalent of DIB, at 50 °C, providing cyclopropane **5** in 48% after 3 h. The online reaction monitoring was carried out with unoptimized conditions in $CDCl_3$ using the R4 glass reactor coupled with the benchtop NMR setup shown in Figure S2. As the reaction stream was continuously delivered into the NMR detection zone, a series of 1D proton scans were measured at intervals between 5 min and 3 h, generating an NMR array of nine spectra (Figure 7a). After 5 min of reaction time, the predominant species were the starting styrene **2**, α-nitroester **4**, and DIB substrates, and within 1 h, the starting species appreciably decreased, while cyclopropane **5** began to appear. Overlapped peaks of three different resonances appeared in the region of δ_H 3.4−4.7, assigned for the vicinal CH^a on the cyclopropane ring, the CH_2 on the ethyl moiety of **5**, and the CH_2 of the ethyl group of **4**. Those coincided with the appearance of the multiplet at δ_H 2.3−2.6 assigned to the geminal cyclopropyl protons (H^b−C-H^c). Moreover, the cyclization process was better monitored through the evolution of the triplet at δ_H 0.5−1.1, assigned to the CH_3 on the ethyl moiety of **5**. The formation of acetic acid was evident as the singlet at δ_H 2.14 appeared concurrently with the disappearance of the DIB's acetate ligand singlet at δ_H 2.10. This was expected from the DIB due to the strongly electrophilic nature of the iodine in DIB, leading to displacement of acetic acid and iodobenzene byproduct.[18] Although the singlet assigned to the methylene moiety of **4** (δ_H 5.2) overlapped with the CH^e of styrene **2** (δ_H 5.1−5.4), it was nonetheless possible to track it is disappearance. The profile of

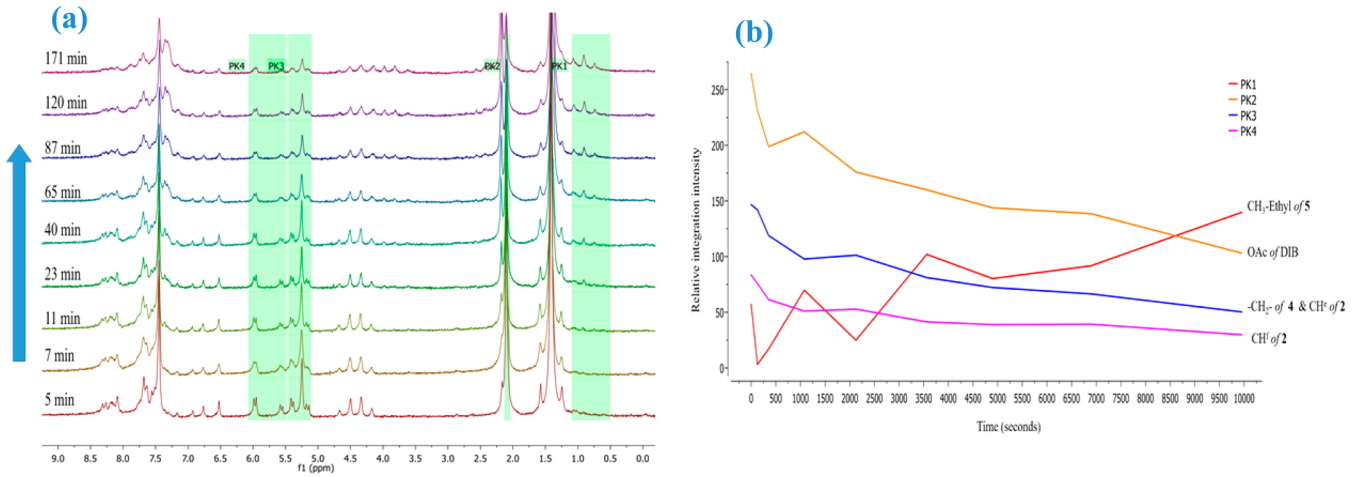

Figure 7. Online monitoring of cyclopropanation of **4** using Spinsolve benchtop NMR (43 MHz): (a) ^{1}H NMR array plot. (b) Profile of reaction progress acquired using the ^{1}H NMR data referenced to selected resonances (Table S3).

DOI: 10.1021/acs.oprd.6b00177
Org. Process Res. Dev. 2016, 20, 1603−1614

the cyclopropanation progress acquired using the ^{1}H NMR data from the nine spectra array clearly demonstrated the progression of the ethyl group on product **5** (δ_H 0.5−1.1) in parallel to the disappearance of the acetate ligands of DIB, the methylene moiety of α-nitroacetate **4** and the geminal protons of styrene **2** (Figure 7b).

3.4. Inline Monitoring of Ethyl-nitroacetate 4 Cyclopropanation under Continuous Process. A continuous flow process for the preparation of the 1-nitro-1-cyclopropylcarboxylate **5**, was developed. Initially the inline monitoring of cyclopropanation of **4** was carried out using the Vaportec R2+/R4 flow system by passing a 0.55 M solution of ethyl-nitroacetate **4** and styrene **2** in DCM along with 0.55 M solution of DIB and catalytic amounts of $Rh_2(esp)_2$ (0.5 mol %) through a heated PTFE coil to provide product **5** in unoptimized 37% yield (Figure 8). The reaction out stream was passed into the solvent evaporation device, to facilitate the exchange of DCM with a total of 4 mL $CDCl_3$ at 35 °C. Upon

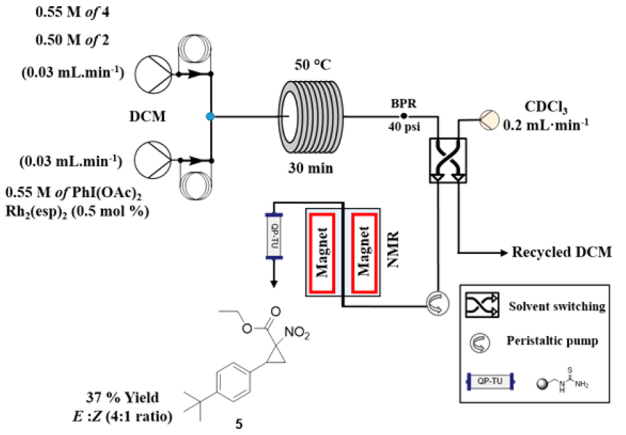

Figure 8. Inline monitoring setup of ethyl-nitroacetate **4** cyclopropanation under flow conditions using the flow-evaporate-analyze protocol.

NMR measurements, the generated steady-state profile for the cyclopropanation of **4** in Figure 9, along with stacked ^{1}H NMR data (Figure S11), demonstrated the partial consumption of the starting species ethyl-nitroacetate **4**, while the formation of cyclopropane **5** was observed by the increased trend assigned for the geminal protons of cyclopropane **5**, along with its ethyl

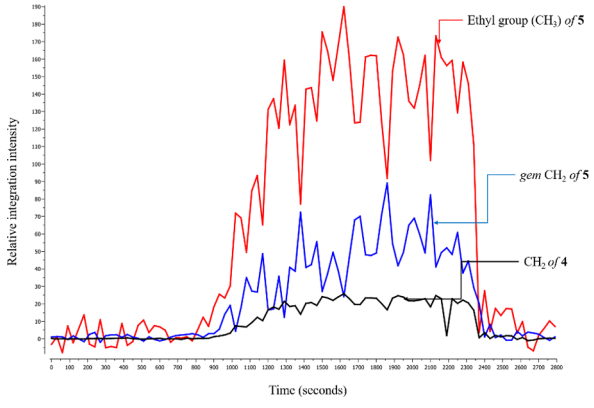

Figure 9. Inline monitoring of cyclopropanation of **4** using Spinsolve benchtop NMR (43 MHz): steady-state profile under flow conditions acquired using the ^{1}H NMR data referenced to selected resonances.

group. As the spectrum was recorded off a crude mixture, the steady state profile appears rather noisy due to the low reaction yield. It is noteworthy that even in nonideal conditions, the steady state is still observed and the product can be tracked. In addition the tracking of the relative integration for the cyclopropane vicinal proton expected at δ_H 3.7, was challenging due to the overlapping with other resonances exhibiting similar chemical shifts. In fact, the ^{1}H NMR spectrum obtained by the inline monitoring of the cyclopropanation of **4**, displayed a number of overlapping signals. Peak overlapping is an inherent problem associated with NMR spectroscopy especially at lower field, however, 2D NMR spectroscopy proved particularly useful in identifying resonances. We demonstrated earlier how the online monitoring of cyclopropanation of malononitrile **1** with Quickcosy facilitated the tracking of correlations between coupled protons under reaction conditions. Likewise, inline monitoring using the Quickcosy for the cyclopropanation of **4** under continuous flow enabled by the use of the Spinsolve automated scripting, allowed more flexibility in monitoring scenarios. Hence, we developed a LEY-2D-COSY script to run a loop sequence of 1D ^{1}H NMR and 2D COSY, executed every 13 min over 3 loops (Figure S12) NMR experiment scripting thus creates tailor-made experimental sequence automation allowing significant time saving and enabling repetitive runs in loops.

The steady-state monitoring of cyclopropanation of **4** with the LEY-2D-COSY script produced three COSY contours along with three 1D proton spectra, demonstrating a number of diagonal and cross correlations (Figures S13 and S14). The presence of unreacted styrene **2** was verified through cross correlations above and below the diagonal line of its olefinic protons at δ_H 5.0−7.2, while the residual substrate of ester **4** appeared with a diagonal peak at δ_H 5.1 assigned to its methylene moiety. Taking a closer look at the COSY horizontal region between δ_H 0.5−5.0 ppm (Figure 10), the formation of cyclopropyl carboxylate **5** was established through its correlation peaks p5 and p5′ due to its vicinal coupling, while the CH_3 and CH_2 protons of cyclopropane **5** ethyl moiety correlated at p1 and p1′. Coupling between the CH_3 and CH_2 protons of the ethyl moiety of **4** was observed by the

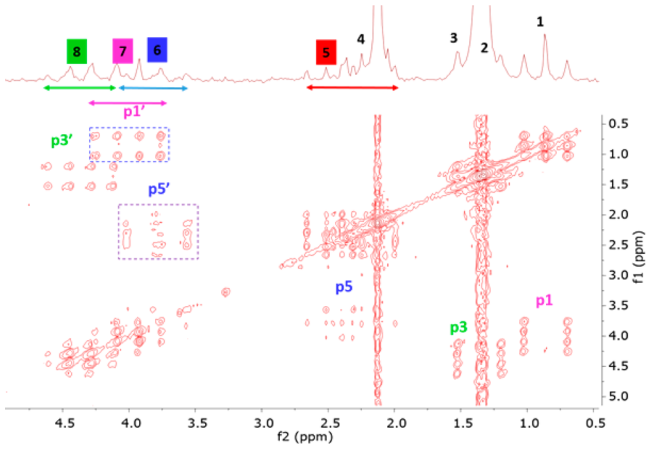

Figure 10. Inline steady-state monitoring of cyclopropanation of **4** with LEY-2D-COSY: 2D COSY contour horizontal region between δ_H 0.5−5 ppm. Resonances: (1) ethyl CH_3 of **5**; (2) *tert*-Butyl of **5** and **2**; (3) ethyl CH_3 of **4**; (4) DIB; (5) geminal CH of **5**; (6) vicinal CH of **5**; (7) ethyl CH_2 of **5**; (8) ethyl CH_3 of **4**. (Further information on the LEY-2D-COSY experiment are found in the Supporting Information.)

DOI: 10.1021/acs.oprd.6b00177
Org. Process Res. Dev. 2016, 20, 1603−1614

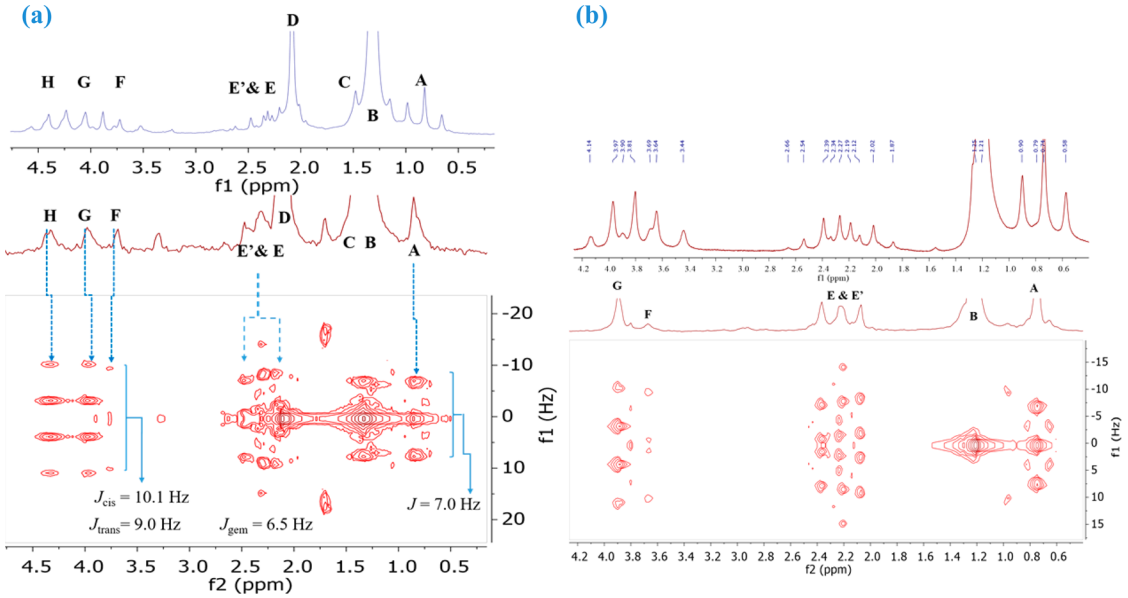

Figure 11. (a) ^{1}H *J*-RES spectrum at 0.5−5.0 ppm of cyclopropanation reaction of **4** crude mixture, with proton signals marked A to H. (b) ^{1}H *J*-RES spectrum of isolated [*E*] 1-nitro-1-cyclopropylcarboxylate **5**. (For ^{1}H *J*-RES of isomer [*Z*] of **5** refer to Figure S 15.) Resonances: (A) ethyl CH_3 of **5**; (B) *tert*-butyl of **5**; (C) ethyl CH_3 of **4**; (D) DIB; (E and E′) geminal CH of **5**; (F) vicinal CH of **5**; (G) ethyl CH_2 of **5**; (H) ethyl CH_3 of **4**.

appearance of cross peaks p3 and its pair p3′. The overlapped peaks in the region of δ_H 3.4−4.7, corresponded to the cross peaks over the COSY contour p1′, p3′, and p5′, and on a closer observation of those cross peaks the extent of overlapping was clarified to be over a portion of 0.5 ppm wide. Similarly, the geminal protons on the cyclopropane **5** were found overlapping with the unreacted acetate peak of DIB over a portion of 0.25 ppm wide. Reaction monitoring using the 2D ^{1}H NMR, in summary, allowed us to clearly distinguish and track starting species consumption and product formation in regions of signal overlap, otherwise unsolvable by 1D ^{1}H NMR.

An additional 2D NMR *J*-resolve spectroscopy (^{1}H *J*-RES) experiment was used for the deconvolution of regions of peak overlap. In *J*-RES the chemical shift and spin−spin coupling are separated, therefore allowing a spin−spin coupling constant *J* (Hz) plot against chemical shift δ_H (ppm). As a result, the signal multiplicity observed in the 1D proton NMR coalesces into a peak in the chemical shift coordinate (horizontal); the signal multiplicity information, however, is transferred into the vertical axis (*J* in Hz). Hence overlapped multiplet signals should coalescence separately, resulting in a discrete set of broader signals, according to their specific resonance environment. The 2D *J*-RES spectrum in the region of 0.5−5.0 ppm shown in Figure 11a, corresponds to the signals of the crude flow mixture from the cyclopropanation reaction of **4**, with proton signals marked A to H. Resonance A, a triplet on the 1D NMR spectrum, was coalescing into a singlet on the *J*-RES horizontal axis, with J = 7.0 Hz, assigned to the CH_3 of ethyl group of **5**. On the other hand, overlapped resonances at δ_H 3.5−4.7, appeared all resolved into three distinct singlets of resonances (F, G, H) on the horizontal axis of the *J*-RES spectrum, where those marked as G and H corresponded to the CH_2 moiety of the ethyl group of **4** and **5**, respectively. The remaining resonance F on the *J*-RES assigned to the cyclopropane ring CH^a proton, appearing as a doublet of doublet in the 2D spectrum. From this doublet of doublet the vicinal couplings was deduced for CH^a with J_{cis} = 10.1 Hz and J_{trans} = 9.0 Hz, in line with the expectation of $J_{cis} > J_{trans}$ for a cyclopropane ring due to the rigid dihedral angle. Moreover the ring rigidity and the substituent effect on the cyclopropane **5** was found to have a positive effect on the geminal coupling between CH^b and CH^c to give J_{gem} of 6.5 Hz, extracted from the two singlets of resonances E and E′ (Figure 11). Furthermore, carrying the *J*-RES measurement of the isolated isomer *E* (major) and isomer *Z* (minor) of 1-nitro-1-cyclopropylcarboxylate **5**, we were also able to observe the differences in chemical shifts between both isomers as demonstrated in Figures 11b and S15, respectively. The distinction in the NMR spectra between the *E* and *Z* isomer was attributed to the orientation of the aryl group with respect to the nitro moiety on the cyclopropane ring. The CH^a signal of the *E* isomer overlapped with the CH_2 of the ethyl group, while both the geminal protons CH^b and CH^c forms a multiple of overlapped peaks between 2.0 and 2.6 ppm (Figure 11b). On the other hand the steric compulsion by the aryl group and the anisotropic effect by the nitro group on the *Z* isomer of cyclopropane **5** caused the ethyl ester group to shift downfield, in comparison to the *E* isomer, whereas both CH^a and CH^b were mildly more shielded, and the CH^c (now *trans* to CH^a) slightly shifted to downfield. It appeared that the *J*-RES of the *E* isomer was visually similar to that of the cyclopropanation reaction crude, confirming that the *E* isomer of **5** was the predominant isomer in the reaction mixture. Hence, through this example, the *J*-RES demonstrated its potential in providing an insightful feedback helping to refine and improve reaction monitoring further.

Further optimization of the cyclopropanation reaction of ethyl-nitroacetate **4** with an equimolar amount of styrene **2** under continuous flow was sought, following the initial 37% yield obtained for cyclopropane **5** (*E* and *Z* combined). This moderate yield was attributed to the high dilution conditions of the reaction, as literature methods highlight the importance of using alkene in excess, with reactions carried out under neat conditions. Several attempts at improving the reaction conditions were made, namely (i) increasing the reaction temperature, (ii) increasing the overall reaction concentration,

DOI: 10.1021/acs.oprd.6b00177
Org. Process Res. Dev. 2016, 20, 1603−1614

and (iii) increasing the number of equivalent of DIB alone (*ditto*), with no success due to low solubility of DIB. However, by flowing an equimolar solution of styrene **2** in DCM along with Rh(II) through an Omnifit column prepacked with 2.2 equiv of solid DIB and 1 mm recyclable glass beads, cyclopropane **5** was afforded in 77% yield (*E*:*Z*, 4:1), over 30 min residence time. Reaction setup under continuous flow is illustrated in Figure 12.

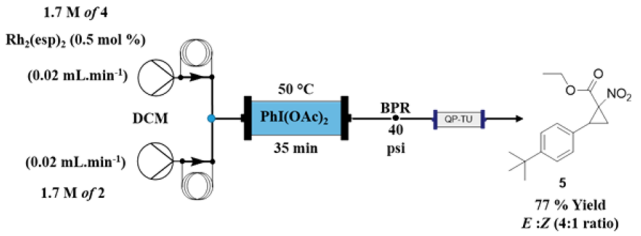

Figure 12. Flow reaction setup for cyclopropanation of **4** under optimized reaction conditions.

3.5. Multiple Monitoring Technique for Cyclopropanation of Phenyl Iodonium Ylide 6 Using CMS-NMR. A multiple monitoring technique approach, using compact mass spectrometry with benchtop NMR (CMS-NMR), was developed in order to provide complementary analytical information for the cyclopropanation of phenyl iodonium ylide. Phenyl iodonium ylide derivatives are widely used in carbene-transfer reactions including cyclopropanation, presenting a comparable reactivity to their diazo counterparts under milder conditions.[19] The iodonium ylide method takes advantage of the readily generated carbene species, induced by metal catalysis, displacing the molecular iodobenzene which then cyclizes in the presence of an olefin. However, it has been established that the iodonium ylide can also provide dimerization products via the competing decomposition of carbene intermediate.[20] As further discussed within, mass spectrometry provided a better insight into the occurrence of such decomposition, compared to NMR which proved challenging with resonance signal overlap. In addition, while NMR monitoring could help to monitor the cyclopropanation of the olefin moiety, the MS could also help to identify the iodobenzene byproduct formation. A continuous process was set for the phenyl iodonium ylide **6** mediated cyclopropanation using the Vaportec R2+/R4 flow system configured with the Spinsolve benchtop NMR and the Advion compact MS with atmospheric pressure chemical ionization (APCI) detector (Figure S18). Using this combined CMS-NMR setup, the cyclopropanation of phenyl iodonium ylide **6** with 4-*tert*-butylstyrene **2** was carried out under continuous flow in the presence of Rh(II) catalyst, to afford cyclopropane-1,1-dicarboxylate **7** (Scheme 3). Ylide **6** was prepared from the reaction of dimethylmalonate **8** with DIB under alkaline conditions in dry acetonitrile, and obtained as an amorphous solid in 65% of crude, without further purification to avoid decomposition of the ylide (Scheme 4).

Scheme 3. Hypervalent Iodine(III) Mediated Synthesis of Cyclopropane-1,1-dicarboxylate 7

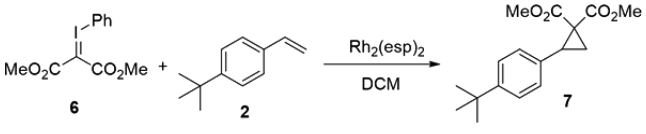

Scheme 4. Synthesis of Phenyl Iodonium Ylide 6

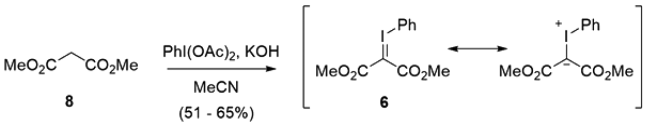

Due to the poor solubility of phenyl iodonium ylide **6** in DCM, we opted for the prepacking into an Omnifit glass column along with 1 mm recyclable glass beads, moreover preventing the caking of the ylide over time. The reaction successfully took place by introducing DCM solution of styrene **2** along with a solution of 0.1 mol% $Rh_2(esp)_2$, through the prepacked column of ylide **6** over 33 min while cooled at 18–20 °C (Figure 13). The ylide gradually consumed and

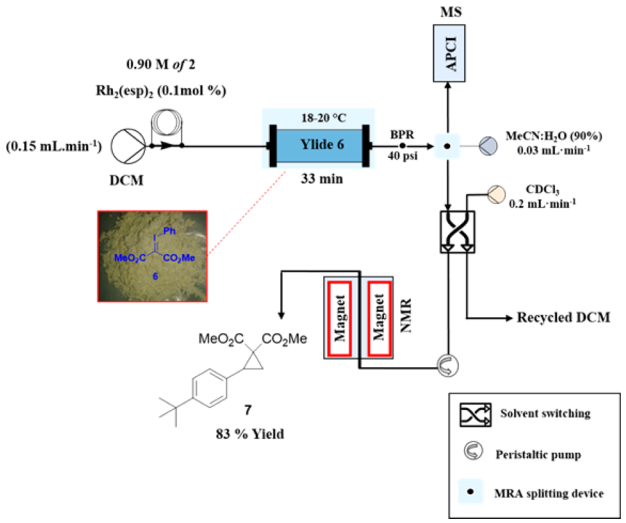

Figure 13. Multiple reaction monitoring setup for the cyclopropanation of ylide **6** under flow conditions.

disappeared from the prepacked column as the styrene **2** solution is streamed through, leaving behind the glass beads. An aliquot of the reaction outflow was periodically redirected to the MS detector zone by mean of a Rheodyne MRA splitting device, while most of the reaction stream output was enriched with deuterated chloroform by passing through the evaporator, prior to NMR analysis. From the resultant MS measurements, the cyclopropane adduct was identified by the molecular ion peak at *m*/*z* 291 [M+H] accompanied by its fragment peak at *m*/*z* 259, while the iodobenzene byproduct was identified at *m*/*z* 204 [M+H] (Figure S20). Cyclopropane **7** formation was also identified using ^{1}H NMR monitoring by the presence of the two dimethoxy moieties that appeared as two separate singlets approximately at δ_H 3.0 and 3.4, as opposed to the dimethoxy moieties of the starting iodonium ylide **6** expected as a one singlet at 3.5 ppm (Figures S21 and S22).

Although ylide **6** demonstrated limited solubility in the reaction medium, however, leaching of the excess ylide from the prepacked column was detectable with the MS by its molecular ion fragment observed at 229 *m*/*z*, while the ylide **6** molecular ion [M+H] was not observed under the APCI conditions (Figure S24). Additionally, the competing decomposition pathway of ylide **6** via dimerization was best

DOI: 10.1021/acs.oprd.6b00177
Org. Process Res. Dev. 2016, 20, 1603−1614

established by MS rather than NMR due to potential signal overlap, with product and ylide, in the region of δ_H 3.5−3.9. This decomposition was demonstrated by the controlled reaction carried in the presence of Rh(II) catalyst where upon MS analysis the molecular ion [M+H] was identified at m/z 261 (Figure S23). When mass monitoring of the cyclopropanation reaction carried at 18−20 °C, on the other hand, no dimerization was observed proving the decomposition pathway did not take place.

3.6. Scope of Hypervalent iodine(III) cyclopropanation under Continuous Flow Conditions. Finally, the potential of the continuous process of these cyclopropanations were further explored at preliminarily level by studying the overall profile of all discussed substrates, malononitrile **1**, ethylnitroester **4**, and phenyl iodonium ylide **6**, with a number of styrene derivatives to afford substituted cyclopropanes in moderate to good yields (Table 1). The best cyclopropanation

Table 1. Cyclopropanation of 1, 4, and 6

Entry	Substrate	Yield[c] (E:Z)[b]
1 (3)	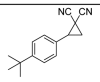	64 %
2 (9)		45 %
3(10)[a]		52 %
4(5)	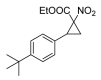	77 % (4.5:1)
5 (11)		43 % (3.7:1)
6 (12)		50 % (4.3:1)
7 (13)		37 % (3.3:1)
8 (7)	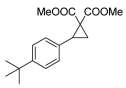	83 %
9 (14)[a]	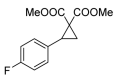	79 %

[a]Reaction carried out at rt. [b]isomer ratio determined by ^{1}HNMR. [c]Isolated yield (unoptimized).

yields were observed with the 4-*tert*-butylstyrene, while lower yields observed with the styrene derivatives bearing electron withdrawing groups. Moreover, a couple of trends emerged with respect to reaction parameters. Although we observed that higher reaction concentration generally improves the productivity, however, excessive concentration can favor substrate decomposition in the case of the malononitrile reactions. Further challenges of achieving optimal reaction concentration in flow were due to reagent limited solubility in the case of DIB. This problem can be eliminated by use of polymer supported DIB reagents or by enhancing solubility with ring functionalization such as *o*-alkoxyphenyliodonium derivatives.[21] A similar balance is found with reaction temperature which, while generally favoring reactivity, can also create polymerization of some styrene substrates at higher temperatures especially when bearing an electron withdrawing group. These preliminary studies generally demonstrate the potential of the hypervalent iodine(III) mediated cyclopropanation continuous process.

CONCLUSION

In conclusion we have reported the efficient use of state-of-the-art benchtop NMR technology for online monitoring of reaction progress over time, and inline tracking of the steady-state of continuous flow processes. Despite the lower field of the reported benchtop NMR, surprisingly useful information arises as a result of the high-homogeneity permanent magnet design, and the efficient reaction monitoring hardware and software interface. A number of hypervalent iodine(III) mediated cyclopropanation reactions were studied to provide a good example of *in situ* monitoring of carbon−carbon bond formation reaction. We made use of combination of one-dimensional and two-dimensional NMR spectroscopy by use of techniques such as COSY to monitor correlations between protons, and *J*-RES to improve reaction monitoring by resolving resonance overlap in the one-dimensional spectrum. In particular, automated scripting of NMR experiments to create customized monitoring scenarios added another dimension to reaction control and study, clearly demonstrating the future potential of benchtop NMR technology as a highly versatile and sophisticated monitoring tool. Moreover, access to real-time numerical data from reaction monitoring offers the clear advantage of enabling decision making within seconds of data acquisition by acting as triggers during computer controlled processes to facilitate reaction optimization. The benchtop technology also proved its adaptability in interfacing with other enabling tools. In particular, we successfully addressed the requirement for the use of deuterated media by developing an efficient solvent switching system integrated with the benchtop NMR. Finally, coupling with mass spectrometry highlighted the effectiveness of the multiple technique approach to provide a multiangle perspective to process understanding and control, in accord with ongoing advances in analytical techniques providing new sophisticated applications increasingly moving toward miniaturized and hybrid monitoring systems with unprecedented perspectives into real-time monitoring.

EXPERIMENTAL SECTION

5.1. Online Monitoring of Malononitrile 1 Cyclopropanation. Based on the online configuration setup described in "reaction monitoring system and methods" (Figure S2). A mixture of $PhI(OAc)_2$ (708 mg, 2.2 mmol), K_2CO_3 (304.0 mg, 2.2 mmol), malononitrile (80 mg, 1.2 mmol), and 4-*tert*-butylstyrene **2** (182 μL, 1.0 mmol) was placed and dissolved with $CDCl_3$ (4.5 mL) in an oven-dried R4 glass reactor fitted into a Vaportec R4 unit, under argon. The resultant reaction mixture was streamed through the NMR at 0.2 mL·min^{-1} set to measure a series of 1D and 2D proton NMR in intervals, while circulating the reaction mixture from and to the reactor, stirred at 50 °C. After completion, the crude mixture was cooled to ambient temperature followed by extraction with DCM (2 × 10 mL) upon an aqueous wash, then

DOI: 10.1021/acs.oprd.6b00177
Org. Process Res. Dev. 2016, 20, 1603−1614

concentrated and purified by flash chromatography using 10% EtOAc:hexane to give **3** as a white solid in 79% yield.

5.2. Inline Monitoring of Malononitrile 1 Cyclopropanation Continuous Process. The following solutions were prepared: (i) a mixture of malononitrile (40 mg, 0.6 mmol) with 4-*tert*-butylstyrene **2** (91 μL, 0.5 mmol) in dry DCM (2 mL); and (ii) $PhI(OAc)_2$ (354 mg, 1.1 mmol) in dry DCM (2.0 mL). Using a Vaportec R2+/R4 flow system, both solutions were individually loaded into 2 mL PFA loops, then delivered simultaneously at flow rates of 0.05 mL·min^{-1} each, through an Omnifit column (4.5 mL) containing K_2CO_3 (2.0 g, 14.5 mmol) with 1 mm-sized glass beads, fitted with 40 psi back pressure regulator, and heated at 60 °C over 44 min residence time. The reaction flow output was directed into the solvent switching device at a flow rate of 0.1 mL·min^{-1}, into the evaporation chamber heated at 45 °C to exchange with $CDCl_3$ (4 mL) at 0.2 mL·min^{-1}, while using air flow at 138 mL·min^{-1}. The concentrated crude in deuterated chloroform was then streamed into the benchtop NMR at 0.2 mL·min^{-1} using Ismatec digital peristaltic pump, set to measure a series of 1D proton NMR in intervals. The crude mixture was concentrated under reduced pressure and the residue was purified by flash chromatography with 10% EtOAc:hexane providing cyclopropane **3** as a white solid in 64% yield.

5.3. Online Monitoring of Ethyl-nitroacetate 4 Cyclopropanation. Based on the online configuration setup described in "reaction monitoring system and methods" (Figure S2). A mixture of $PhI(OAc)_2$ (800 mg, 2.4 mmol), $Rh_2(esp)_2$ (8 mg, 0.5 mol %), ethyl-nitroacetate **4** (243 μL, 2.2 mmol), and 4-*tert*-butylstyrene **2** (354 μL, 2.2 mmol) was placed and dissolved with $CDCl_3$ (4.5 mL) in an oven-dried R4 glass reactor fitted into a Vaportec R4 unit, under argon. The resultant reaction mixture was streamed through the NMR at 0.2 mL·min^{-1} set to measure a series of 1D proton NMR in intervals, while circulating the reaction mixture from and to the reactor stirred at 50 °C. The resulting crude mixture was filtered through a PS-TU (500 mg, 3.2 mmol·g^{-1}), concentrated, and purified by flash chromatography using 5% EtOAc:hexane to give cyclopropane adduct **5** as pale yellow oil in 39−48% yield.

5.4. Inline Monitoring of Ethyl-nitroacetate 4 Cyclopropanation Continuous Process. The following solutions were prepared: (i) a mixture of ethyl-nitroacetate **4** (122 μL, 1.1 mmol) with 4-*tert*-butylstyrene **2** (177 μL, 1 mmol) in dry DCM (2 mL); and (ii) $PhI(OAc)_2$ (354 mg, 1.1 mmol) with $Rh_2(esp)_2$ (4 mg, 0.5 mol%) in dry DCM (2 mL). Using a Vaportec R2+/R4 flow system, both solutions were individually loaded into 2 mL PFA loops which then delivered simultaneously through 2 mL PTFE flow coil, fitted with 40 psi back pressure regulator, heated at 50 °C over 30 min residence time. The reaction flow output was directed into the solvent switching device at a flowing rate of 0.06 mL·min^{-1} into the evaporation chamber heated at 35 °C, to exchange with $CDCl_3$ (4 mL) at 0.2 mL·min^{-1}, while using air flow at 138 mL·min^{-1}. The concentrated crude in deuterated chloroform was then streamed into the benchtop NMR, set to carry a series of 1D or 2D proton NMR experiments in intervals. As the flow output emerged from the NMR, the crude solution was filtered through a prepacked column of PS-TU (500 mg, 3.2 mmol·g^{-1}), concentrated, and purified with flash chromatography using 5% EtOAc:hexane to give **5** in 37% yield as a light yellow oil of *E* and *Z* isomer combined (4:1 ratio).

5.5. Optimized Continuous Condition for Cyclopropanation of Ethyl-nitroacetate 4. The following solutions were prepared: (i) a mixture of ethyl-nitroacetate **4** (188 μL, 1.7 mmol), and $Rh_2(esp)_2$ (6.6 mg, 0.5 mol%) in dry DCM (1 mL); and (ii) 4-*tert*-butylstyrene **2** (312 μL, 1.7 mmol) in dry DCM (1 mL). Using a Vaportec R2+/R4 flow system, both solutions were individually loaded into 1 mL PTFE loops, which then delivered simultaneously at 0.02 mL·min^{-1} each, through an Omnifit column (1.4 mL) containing $PhI(OAc)_2$ (1.2 g, 3.7 mmol) with 1 mm-sized glass beads, heated at 50 °C over 35 min. After passing the back pressure regulator (40 psi), the flow output was streamed through a prepacked column of PS-TU column (1 g, 3.2 mmol·g^{-1}). The collected crude mixture was concentrated under reduced pressure and purified by flash chromatography using 5% EtOAc:hexane providing cyclopropane adduct **5** as a light yellow oil in 77% yield of *E* and *Z* isomer combined (4:1 ratio).

5.6. Synthesis of bis(Methoxycarbonyl)-(phenyliodinio) Methanide Ylide 6. In a 100 mL oven-dried flask under argon cooled to 0 °C, were added pellets of potassium hydroxide (3.0 g, 45 mmol), dry MeCN (30 mL) followed by dimethyl malonate (1.0 mL, 9 mmol). The resulting milky suspension mixture was then stirred for 5 min at 0 °C, before addition of $PhI(OAc)_2$ (3.2 g, 9.9 mmol). The reaction mixture was left to stir for 3 h at 0 °C leading to a thick and creamy colored mixture. After reaction, H_2O (15 mL) was added and left to stir for 2 min, followed by filtration of the fluffy suspension under vacuo. The solid was then washed with H_2O (10 mL × 2), followed by Et_2O (10 mL), then left to dry under vacuum for 15 min and dried under high vacuum overnight providing iodonium ylide **6** in 51−65% crude yields as a cream to white solid with no further purification.

5.7. Inline Monitoring of Cyclopropanation Continuous Process of Ylide 6. Using the Vaportec R2+/R4 flow system, a solution of 4-*tert*-butylstyrene (338 μL, 1.8 mmol) and $Rh_2(esp)_2$ (2 mg, 0.1 mol%, w.r.t ylide) in dry DCM (2 mL), was loaded into 2 mL PFA loop which was then streamed at 0.15 mL·min^{-1} through an Omnifit column (5 mL) containing phenyl iodonium ylide **6** (730 mg, 2 mmol) with 1 mm-sized glass beads, over 33 min residence time at 18−20 °C using water-ice bath. The reaction stream output, was sampled to the Advion compact mass spectrometer using the Rheodyne MRA splitting device (4-ports) to periodically sample the postflow stream with split ratio mark 4 (500:1) using HPLC carrier solvent mixture of MeCN:H_2O (90% with 1% formic acid) at flow rate 0.03 mL·min^{-1}. The remaining reaction stream output was directed into the evaporation chamber at 30 °C, to exchange with $CDCl_3$ (5 mL) at 0.2 mL·min^{-1}, while using air flow at a rate of 150 mL·min^{-1}. The crude in deuterated chloroform was then streamed through the benchtop NMR, using the PTFE NMR cell, to carry a series of 1D proton NMR experiments. The collected crude solution was then filtered through a PS-TU (500 mg, 3.2 mmol·g^{-1}), concentrated, and purified using flash chromatography with 10% EtOAc:hexane to afford cyclopropane 1,1-dicarboxylate **7** as a colorless oil in 83% yield.

■ ASSOCIATED CONTENT

Supporting Information

The Supporting Information is available free of charge on the ACS Publications website at DOI: 10.1021/acs.oprd.6b00177.

DOI: 10.1021/acs.oprd.6b00177
Org. Process Res. Dev. 2016, 20, 1603−1614

Characterization of compounds, additional details of reaction monitoring methods and setup, and data archive[22] (PDF)

AUTHOR INFORMATION

Corresponding Author

*Email: batoolahmedomer@gmail.com.

Funding

University of Cambridge funding Daphne Jackson Fellowship (B.A.O.); iCON funding RG74817 through CMAC (E.S.); UK Engineering and Physical Sciences Research Council, Critical Mass grant (EPSRC, EP/K009494K/1), the EPSRC Core Capability grant (EPSRC grant EP/K039520/1) (E.S and S.V.L.).

Notes

The authors declare the following competing financial interest(s): John Paul Cerroti declares that he is employed by Magritek GmbH, the supplier of the benchtop NMR instrument used in this study.

ACKNOWLEDGMENTS

The authors gratefully acknowledge the support of Daphne Jackson Trust for the Daphne Jackson Fellowship funded by the University of Cambridge (B.A.O.), CMAC (E.S.), and UK Engineering and Physical Sciences Research Council Critical Mass grant and the EPSRC Core Capability grant.

ABBREVIATIONS

^{1}H NMR, proton nuclear magnetic resonance; COSY, correlation spectroscopy; *J*-RES, *J*-resolved spectroscopy; CMS, compact mass spectroscopy; RM, reaction monitoring

REFERENCES

(1) (a) Zhou, F. X.; Bertels, T. *J. Bus. Chem.* **2014**, *11*, 33−42. (b) Barnhart, T. M. *Creating a Lean R&D System*; Taylor & Francis Group, Boca Raton: FL, 2013.

(2) Yu, L. X. *Pharm. Res.* **2008**, *25*, 781−791.

(3) Anastas, P. T.; Warner, J. C. *Green Chemistry: Theory and Practice*; Oxford University Press: New York, 1998.

(4) Chanda, A.; Daly, A. M.; Foley, D. A.; LaPack, M. A.; Mukherjee, S.; Orr, J. D.; Reid, G. L.; Thompson, D. R.; Ward, H. W. *Org. Process Res. Dev.* **2015**, *19*, 63−83.

(5) (a) Ferreira, A. P.; Tobyn, M. *Pharm. Dev. Technol.* **2015**, *20* (5), 513−527. (b) Houben, C.; Lapkin, A. A. *Curr. Opin. Chem. Eng.* **2015**, *9*, 1−7.

(6) (a) Fitzpatrick, D. E.; Battilocchio, C.; Ley, S. V. *Org. Process Res. Dev.* **2016**, *20* (2), 386−394. (b) Holmes, N.; Akien, G. R.; Savage, R. J. D.; Stanetty, C.; Baxendale, I. R.; Blacker, A. J.; Taylor, B. A.; Woodward, R. L.; Meadows, R. E.; Bourne, R. A. *React. Chem. Eng.* **2016**, *1*, 96−100. (c) Moore, J. S.; Jensen, K. F. *Org. Process Res. Dev.* **2012**, *16*, 1409−1415. (d) Rasheed, M.; Wirth, T. *Angew. Chem., Int. Ed.* **2011**, *50*, 357−358. (e) McMullen, J. P.; Jensen, K. F. *Org. Process Res. Dev.* **2010**, *14*, 1169−1176.

(7) (a) Roscioli, K. M.; Zhang, X.; Li, S. X.; Goetz, G. H.; Cheng, G.; Zhang, Z.; Siems, W. F.; Hill, H. H., Jr *Int. J. Mass Spectrom.* **2013**, *336*, 27−36. (b) Browne, D. L.; Wright, S.; Deadman, B. J.; Dunnage, S.; Baxendale, I. R.; Turner, R. M.; Ley, S. V. *Rapid Commun. Mass Spectrom.* **2012**, *26*, 1−12. (c) Carter, C. F.; Lange, H.; Baxendale, I. R.; Wittkamp, B.; Goode, J. G.; Gaunt, N. L.; Ley, S. V. *Org. Process Res. Dev.* **2010**, *14* (2), 393−404. (d) Marziano, I.; Sharp, D. C. A.; Dunn, P. J.; Hailey, P. A. *Org. Process Res. Dev.* **2000**, *4*, 357−361.

(8) (a) Sans, V.; Porwol, L.; Dragone, V.; Cronin, L. *Chem. Sci.* **2015**, *6*, 1258−1264. (b) Foley, D. A.; Bez, E.; Codina, A.; Colson, K. L.; Fey, M.; Krull, R.; Piroli, D.; Zell, M. T.; Marquez, B. L. *Anal. Chem.* **2014**, *86*, 12008−12013. (c) Foley, D. A.; Wang, J.; Maranzano, B.; Zell, M. T.; Marquez, B. L.; Xiang, Y.; Reid, G. L. *Anal. Chem.* **2013**, *85*, 8928−8932.

(9) (a) Parker, T.; Limer, E.; Watson, A. D.; Defernez, M.; Williamson, D.; Kemsley, E. K. *TrAC, Trends Anal. Chem.* **2014**, *57*, 147−158. (b) Pagès, G.; Gerdova, A.; Williamson, D.; Gilard, V.; Martino, R.; Malet-Martino, M. *Anal. Chem.* **2014**, *86*, 11897−11904. (c) Dalitz, F.; Cudaj, M.; Maiwald, M.; Guthausen, G. *Prog. Nucl. Magn. Reson. Spectrosc.* **2012**, *60*, 52−70. (d) Gouilleux, B.; Charrier, B.; Danieli, E.; Dumez, J.-N.; Akoka, S.; Felpin, F.-X.; Rodriguez-Zubiri, M.; Giraudeau, P. *Analyst* **2015**, *140*, 7854−7858.

(10) *Online benchtop NMR reaction monitoring*: http://www.magritek.com/wp-content/uploads/2015/12/Magritek-Spinsolve-ReactionMonitoring-Brochure-Dec-1-2015-web.pdf (last visited May 15, 2016).

(11) (a) Foley, D. A.; Zell, M. T.; Dunn, A. L. *Magn. Reson. Chem.* **2016**, *5*445110.1002/mrc.4259. (b) Moore, J. S.; Jensen, K. F. *Angew. Chem., Int. Ed.* **2014**, *53*, 470−473.

(12) Deadman, B. J.; Battilocchio, C.; Sliwinski, E.; Ley, S. V. *Green Chem.* **2013**, *15*, 2050−2055.

(13) Wirth, T.; Altermann, S.; Biland, A. S. *ARKIVOC* **2003**, *vi*, 164−169.

(14) Lin, S.; Li, M.; Dong, Z.; Liang, F.; Zhang, J. *Org. Biomol. Chem.* **2014**, *12*, 1341−1350.

(15) (a) Gouilleux, B.; Rodriguez-Zubiri, M.; Felpin, F.-X.; Akoka, S.; Dumez, J.-N.; Danieli, E.; Charrier, B.; Giraudeau, P *Analyst* **2015**, *140*, 7854−7858. (b) Giraudeau, P.; Frydman, L. *Annu. Rev. Anal. Chem.* **2014**, *7*, 129−61. (c) Zhang, Z.; Smith, P. E. S.; Frydman, L. *J. Chem. Phys.* **2014**, *141*, 194201. (d) For Quickcosy please visit http://www.magritek.com/.

(16) (a) Moreau, B.; Charette, A. B. *J. Am. Chem. Soc.* **2005**, *127*, 18014−18015. (b) Wurz, R. P.; Charette, A. B. *Org. Lett.* **2003**, *5* (13), 2327−2329.

(17) Wurz, R. P.; Charette, A. B. *J. Org. Chem.* **2004**, *69*, 1262−1269.

(18) Wirth, T.; Ochiai, M.; Varvoglis, A.; Zhdankin, V. V.; Koser, G. F.; Tohma, H.; Kita, Y. *Topics in Current Chemistry: Hypervalent Iodine Chemistry: Modern Developments in Organic Synthesis*; Springer-Verlag: Berlin, 2002.

(19) Muller, P.; Fernandez, D. *Helv. Chim. Acta* **1995**, *78*, 947−958.

(20) (a) Goudreau, S. R.; Marcoux, D.; Charette, A. B. *Org. Synth.* **2010**, *87*, 115−125. (b) Pomerantz, M.; Levanon, M.; Xiaomin, G.; Dias, H. V. R. *Tetrahedron* **1997**, *53* (29), 10019−10028.

(21) (a) Zhu, C.; Yoshimura, A.; Ji, L.; Wei, Y.; Nemykin, V. N.; Zhdankin, V. V. *Org. Lett.* **2012**, *14* (12), 3170−3173. (b) Ley, S. V.; Baxendale, I. R.; Brusotti, G.; Caldarelli, M.; Massi, A.; Nesi, M. *Farmaco* **2002**, *57*, 321−330. (c) Ley, S. V.; Thomas, A. W.; Finch, H. *J. Chem. Soc., Perkin Trans. 1* **1999**, *1*, 669−671.

(22) Ahmed-Omer, B.; Sliwinski, E.; Cerroti, J. P.; Ley, S. V. *Continuous Processing and Efficient In Situ Reaction Monitoring of a Hypervalent Iodine (III) Mediated Cyclopropanation using Benchtop NMR Spectroscopy*; University of Cambridge data repository; http://dx.doi.org/10.17863/CAM.605, 2016. (accessed Aug 06, 2016).

DOI: 10.1021/acs.oprd.6b00177
Org. Process Res. Dev. 2016, 20, 1603−1614